Energy Science & Engineering

Open Access

RESEARCH ARTICLE

Field testing of thermoplastic encapsulants in high-temperature installations

Michael D. Kempe[1], David C. Miller[1], John H. Wohlgemuth[1], Sarah R. Kurtz[1], John M. Moseley[1], Qurat A. Shah[2], Govindasamy Tamizhmani[2], Keiichiro Sakurai[1,3], Masanao Inoue[4], Takuya Doi[4], Atsushi Masuda[4], Sam L. Samuels[5] & Crystal E. Vanderpan[6]

[1]National Renewable Energy Laboratory, 15013 Denver West Parkway, Golden, Colorado 80401
[2]Arizona State University Photovoltaic Reliability Laboratory, 7349 East Unity Avenue, Mesa, Arizona
[3]National Institute of Advanced Industrial Science and Technology, 1-1-1 Umezono, Tsukuba, Ibaraki 305-8568, Japan
[4]National Institute of Advanced Industrial Science and Technology, 807-1, Shuku-Machi, Tosu, Saga 841-0052, Japan
[5]DuPont Company, 200 Powder Mill Road, Wilmington, Delaware 19803
[6]Underwriters Laboratories, 455 East Trimble Road, San Jose, California

Keywords
Adhesives, creep, encapsulant, polymer, qualification standards, thermoplastic

Correspondence
Michael D. Kempe, National Renewable Energy Laboratory, 15013 Denver West Parkway, Golden, CO 80401. Tel: 303-384-6325; E-mail: michael.kempe@nrel.gov

Funding Information
This work was supported by the U.S. Department of Energy under Contract No. DE-AC36-08-GO28308 with the National Renewable Energy Laboratory.

Received: 27 April 2015; Revised: 23 September 2015; Accepted: 2 October 2015

***Energy Science and Engineering* 2015; 3(6):565–580**

doi: 10.1002/ese3.104

Abstract

Recently there has been increased interest in using thermoplastic encapsulant materials in photovoltaic modules, but concerns have been raised about whether these would be mechanically stable at high temperatures in the field. Recently, this has become a significant topic of discussion in the development of IEC 61730 and IEC 61215. We constructed eight pairs of crystalline-silicon modules and eight pairs of glass/encapsulation/glass thin-film mock modules using different encapsulant materials, of which only two were formulated to chemically crosslink. One module set was exposed outdoors with thermal insulation on the back side in Mesa, Arizona, in the summer (hot-dry), and an identical module set was exposed in environmental chambers. High-precision creep measurements (±20 μm) and electrical performance measurements indicate that despite many of these polymeric materials operating in the melt or rubbery state during outdoor deployment, no significant creep was seen because of their high viscosity, lower operating temperature at the edges, and/or the formation of chemical crosslinks in many of the encapsulants with age despite the absence of a crosslinking agent. Only an ethylene-vinyl acetate (EVA) encapsulant formulated without a peroxide crosslinking agent crept significantly. In the case of the crystalline-silicon modules, the physical restraint of the backsheet reduced creep further and was not detectable even for the EVA without peroxide. Because of the propensity of some polymeric materials to crosslink as they age, typical thermoplastic encapsulants would be unlikely to result in creep in the vast majority of installations.

Introduction

There has been recent interest in the use of thermoplastic encapsulant materials in photovoltaic (PV) modules to replace chemically crosslinked materials, for example, ethylene-vinyl acetate (EVA). The related motivations include the desire to: reduce lamination time or temperature, reduce moisture permeation, use less corrosive materials, improve electrical resistance, or facilitate the reworking of a module during production. However, the use of any thermoplastic material in a high-temperature outdoor environment raises safety and performance concerns. Therefore, there has been increased concern in the PV community regarding the possibility of viscoelastic creep prompting consideration for inclusion of a creep test into IEC 61730 and IEC 61215 [1–3]. Small areas of a module may reach much higher temperatures (>150°C) during the "hot-spot" test or during partial shading of a module without bypass-diode protection [4, 5]; but the localized nature of this occurrence is different from the situation

© 2015 The Authors. *Energy Science & Engineering* published by the Society of Chemical Industry and John Wiley & Sons Ltd.
This is an open access article under the terms of the Creative Commons Attribution License, which permits use, distribution and reproduction in any medium, provided the original work is properly cited.

of prolonged operation in the hottest module operating environments and mounting configurations. In very hot environments, modules are known to reach temperatures in excess of 100°C [6, 7]. One could envision an encapsulant with a melting point near 85°C with a highly thermally activated drop in viscosity, resulting in significant creep at 100°C.

Some early work with EVA encapsulation performed at Jet Propulsion Laboratories (JPL) did consider the issue of displacement during operation at high temperature [1, 8]. PV technology developers at that time speculated at the possibility of the displacement of components within a heated module operating in the field, but did not formally investigate to verify creep using a variety of modules deployed in a hot location. To specifically prevent creep, EVA that was crosslinked via a peroxide-initiated reaction was advocated at that time. The gel-content test was originally used at JPL as a means to quantify the content of insoluble crosslinked gel in EVA. The use of 65% gel was found to facilitate passing the sales qualification tests (which included the "melt/freeze" test at that time) and was therefore recommended by JPL. The use of EVA with at least 65% gel content was reaffirmed by Springborn Laboratories (later known as Specialized Technology Resources, Inc., or STR) [9], and presently, the use of EVA with 60–90% gel content is common in the industry.

The possibility of creep was more formally speculated in quantitative rheometry measurements of encapsulation materials [6, 7], motivating the study described in this paper. Characterization of the displacement from viscoelastic flow, identified here as "creep," should be distinguished from the "creep test" used to characterize the effects of densification associated with the process of physical aging [10]. "Creep" facilitated by prolonged exposure to high temperature is also different from the effects associated with rate-dependent loading [2].

This paper studies the potential hazard associated with creep in modules and how to test for such a problem [11, 12]. Modules fabricated with a variety of encapsulant materials are subjected to high temperatures and the resulting creep is documented as a function of temperature for each encapsulant type. The observed creep is compared with material-level tests to identify the best way to characterize phase transitions that could be predictive of creep in the field. The results are discussed to evaluate the hazard associated with creep for the materials studied and to propose both module- and material-level tests for evaluating the potential for creep. In the Experimental section, we describe the module construction, methods for measuring the phase transitions and rheological properties of the chosen encapsulant materials, modeling studies that were used to design the outdoor deployments, the methodology for the outdoor deployments, the methodology for the step stress applied in environmental chambers, and the technique for measuring creep. In the Results section, we summarize the temperatures that were measured outdoors, the phase transition and rheological data collected for the encapsulant materials, the creep measured outdoors and in the chamber step-stress testing, and the high-pot test results. We also compare the creep measured outdoors and indoors with each other and with the phase transitions and rheological properties measured for the encapsulant materials. Using these observations, we propose a test designed to give confidence that creep rates will be negligible even in the hottest location. We also discuss evidence of material changes that are occurring during these tests. In the section Discussion: Creep and its Consequences, we summarize the conclusions, including the specific recommendation of module- and material-level tests to predict creep for products in the field.

Experimental

Encapsulant materials

Encapsulant materials chosen for this study were obtained from industrial manufacturers and are either being used, or under investigation for use, in PV modules (Table 1). However, without additional formulation-specific information, the product name is not of further use (from a scientific standpoint) in the context of this study. For the polydimethyl siloxane (PDMS) encapsulation, a different formulation was used for the thin-film mock modules than in the crystalline-silicon modules; however, both are sparsely crosslinked gels of similar composition, and the manufacturer of them indicated that they were extremely similar in composition. The PDMS values in Table 1 apply to the thin-film mock modules. Notably, the NC-EVA was formulated identically to a commercial EVA formulation but without the inclusion of a peroxide to promote curing during lamination.

Dynamic mechanical analysis (DMA) was performed on a TA Instruments ARES rheometer. Samples were tested in either a torsional configuration at temperatures below the melt or in a parallel-plate configuration near or above the melt transition. Data in Table 1 were measured at 0.1 rad/sec.

Differential scanning calorimetry (DSC) was performed using a TA Instruments DSC Q1000. Data were taken from the second of two consecutive cycles (from $-100°< T < 200°C$ or $-180°< T < 200°C$ for silicones) at the rate of 10°C/min in an N_2 environment.

Melt flow rate (MFR) measurements were performed on the Dynisco Melt Flow Indexer Model 4002. Testing weights included 0.225 kg, 0.95 kg, 2.06 kg, 4.12 kg (made

 © 2015 The Authors. *Energy Science & Engineering* published by the Society of Chemical Industry and John Wiley & Sons Ltd.

Table 1. Phase transitions determined by differential scanning calorimetry (DSC) and dynamic mechanical analysis (DMA). DMA glass transitions (T_g). DMA melting transitions (T_m) were determined when the phase angle was 45°, or at an inflection point in the modulus when a phase angle of 45° was absent. The crossover temperature (T_c) is where the phase angle of 45° occurs for materials with no melt transition.

		Phase transitions					
		DSC			DMA at 0.1 rad/sec		
Encapsulant material type and designation		T_g (°C)	T_m (°C)	T_f (°C)	T_g (°C)	T_m (°C)	T_c (°C)
Cured commercial PV EVA resin	EVA	−31	55	45	−30	47	
Commercial PV EVA Resin with all components but the peroxide	NC-EVA	−31	65	45	−28	69	
Polyvinyl butyral	PVB	15			17		121
Aliphatic thermoplastic polyurethane	TPU	2			3		84
Pt catalyzed, addition cure polydimethyl silioxane gel (mock modules)	PDMS-M	−158	−40	−80			
Pt catalyzed, addition cure polydimethyl silioxane gel (si modules)	PDMS-Si	−150	−40	−80			
Thermoplastic polyolefin #1	TPO-1	−43	93	81	−35	105	
Thermoplastic polyolefin #3	TPO-3	−44	61	55	−41	79	
Thermoplastic polyolefin #4	TPO-4	−34	106	99	−21	115	

by stacking two 2.06 kg weights), and 9.8 kg weights (made by stacking two 4.9 kg weights). Including the 0.11 kg weight of the piston, the net testing loads were 0.335, 1.06, 2.17, 4.23, and 9.91 kg, respectively. The tungsten carbide die had an orifice diameter of 2.095 ± 0.005 mm. The heating chamber allowed for steady-state temperature control to ±0.1°C.

Si module construction

The first module construction was a functional module with typical crystalline-silicon cells. It contained 42 156-mm multicrystalline, upgraded metallurgical-grade silicon cells with total dimension of 96.8 cm × 114.8 cm, providing an average module efficiency, at standard testing conditions (STC) [13], of 14.7 ± 0.3%. Because of a broken cell, one module had an efficiency of 12.7% and was not considered for this efficiency average. An Al frame was used with 3.18 mm tempered-glass superstrate, and a composite backsheet of Tedlar®-polyethylene terephthalate-Tedlar® (Dupont, Wilmington, Delaware) (TPT) construction. This backsheet composite construction was chosen because it is made of commonly used materials, and because it did not contain a low-vinylacetate, poly EVA seed layer. An EVA seed layer was also thought to be more likely to have adhesion compatibility concerns, whereas Tedlar® is surface treated to provide good adhesion to a wide variety of materials. During the course of this experiment, no delamination of the TPT from any interface was observed.

Because different methods are used for making PDMS encapsulated modules, the PDMS silicon modules were constructed at an outside vendor. Sixty 156-mm, multicrystalline cells with a PET-based backsheet and Al frame were used for the PDMS modules, which had overall dimensions of 166.4 cm × 97.2 cm, and an average efficiency of 13.9 ± 0.7% at STC.

Thermal insulation was mounted to the back of the field-deployed modules to simulate mounting on an insulated roof. This is a realistic mounting configuration, representing the worst-case installation scenario on an insulated roof. Insulation was attached to the back of the module using a piece of 12.5-mm-thick plywood. Metal brackets, attached to the frame and the plywood, provided a gap of about 10 cm between the wood and backsheet. A 2.64 m^2·K/W [R15, 15 (h·ft^2·°F/Btu)] fiberglass mat insulation was inserted between the plywood and backsheet. The sides of the module were covered with duct tape to reduce air circulation around the perimeter and to prevent the insulation from being damaged (Fig. 1).

Thin-film mock module construction

The second module construction was designed to mimic a thin-film module with 61 cm × 122 cm dimensions, with a 3.18-mm-thick glass superstrate and substrate. These thin-film mock modules were not functional, containing only an F:SnO transparent conductive oxide (TCO) layer on the front piece of glass, and no PV cell present. The TCO was removed within 12.7 mm of the perimeter using laser ablation. The TCO was electrically connected to a conductive ribbon through a hole in the back glass to allow evaluation of safety compliance for the "Wet Leakage Current Test" [14, 15]. To mechanically fix and electrically isolate the ribbons during electrical testing, the ribbons were potted in a black silicone (Dow Corning 737).

© 2015 The Authors. *Energy Science & Engineering* published by the Society of Chemical Industry and John Wiley & Sons Ltd.

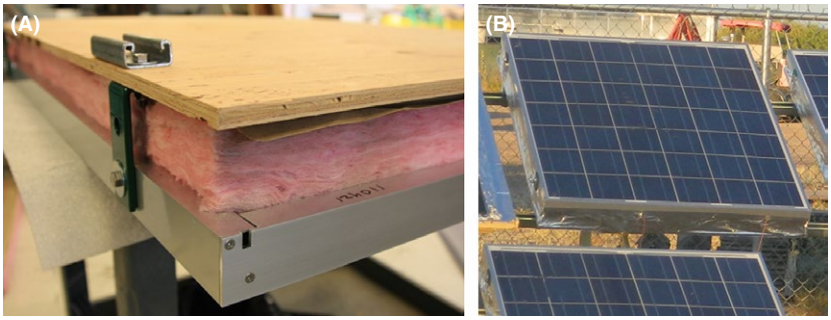

Figure 1. Photos of Si modules (A) during construction (B) as mounted in Mesa, Arizona.

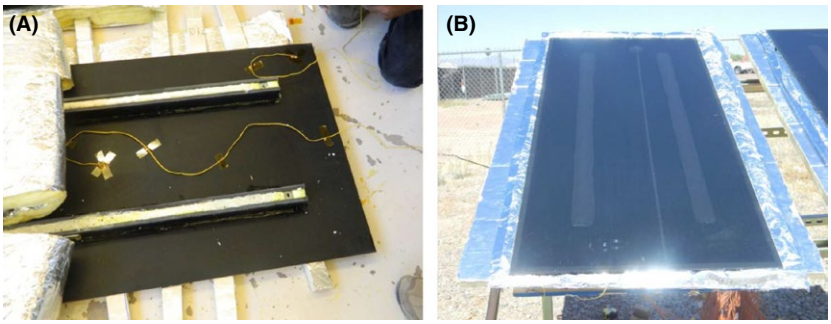

Figure 2. Photos of a thin-film mock module (A) during construction (B) after deployment in Mesa, Arizona.

To give the modules similar light absorptance—and hence, the thermal properties of a thin-film module—the backside of the glass substrate was painted black using Rust-Oleum® (Vernon Hills, Illinois) Universal flat-black enamel spray paint (P/N 245198). The absorptance of light by the paint, measured from the front glass side and weighted against the energy in the global solar spectrum [16], was 89.8%. This value compared favorably with the measured absorptance of representative Si, α-Si, and CdTe modules of 88.3, 87.8, and 89.4%, respectively.

Thin-film mock modules were mounted by adhesively attaching a 4 cm × 4 cm, 91-cm-long Unistrut fiberglass channel (McMaster-Carr, P/N 3261T34) on the back using Dow Corning 737 silicone, allowing the front piece of glass to move freely. No edge seal was present in the mock modules, so that the highest possible shear stress might be encountered. For the outdoor exposed modules, thermal insulation was applied to the back by filling the fiberglass channels with spray-in foam insulation, followed by a layer of 2.54-cm-thick fiberglass mat insulation (1.18 m^2·K/W or R6.7), and a layer of 2.54-cm-thick polyisocyanurate sheeting (1.16 m^2·K/W or R6.6). The two insulation layers were larger in width and height than the module to help reduce thermal gradients across the module, especially near the edges. The insulation had sections cut out to allow it to be placed around the Unistrut channels. The insulation was held in place by a 1.25-cm-thick piece of plywood, attached to the Unistrut channels on the backside, and thus compressed the fiberglass insulation eliminating air flow on the back (Fig. 2).

Module temperature measurement

For these modules, and for the Si modules, K-type thermocouples (accuracy ±1°C) were placed in the center and 6 ± 2 cm from one corner on the backsides of the modules using Kapton tape. Module temperature was recorded at 6-min intervals. Additionally, one thin-film NC-EVA mock module was deployed in Golden, Colorado, and monitored at four locations (bottom-right corner, middle-left, middle-right, and the center) as indicated in Figure 7. Thermal images were also obtained using a FLIR Systems, Inc., ThermaCAM SC640 capable of resolving temperature variations to within 0.06°C.

Outdoor deployment

Modules were deployed at Arizona State University in Mesa, Arizona, from May to September 2011 on a rack inclined at the 33° latitude tilt and a 255° azimuth. This orientation was chosen to achieve the highest maximum module temperature possible. Because tracked systems do

 © 2015 The Authors. *Energy Science & Engineering* published by the Society of Chemical Industry and John Wiley & Sons Ltd.

not have significantly restricted air flow on the back side, they operate at lower temperatures than roof mounted systems and were not considered for this study. This was determined using Typical Meteorological Year (TMY3) [14] data for Phoenix, AZ, along with the module temperature estimation equations from King et al. [17] for an insulated-back module accurate to ±5°C for Si cells. The maximum module temperature as a function of azimuth and tilt angle is shown in Figure 3. The maximum temperature is seen for all inclination angles at a southwest-facing azimuth of 255 ± 5°. For Phoenix in summer, this corresponds to a module facing the sun at 17:00 at the hottest part of the day (typically between 16:00 and 17:00). In Figure 3, there are two distinct peaks at the tilt angles of 28.3° and 34.5°. This can be interpreted as two different times (separated by several weeks) where some significantly hot days occurred and a different tilt angle helps to maximize the temperature. Arizona is at 33.4° latitude, so modules at the site were mounted at 33°, because we could not predict when the hottest days of the summer would occur.

Although the angles shown in Figure 3 demonstrate variability in maximum temperature from 95° to 106°C, the average temperature (including day and night) for a tilt of 33° was 49.03°C and 49.40°C for an azimuth of 180° and 255°, respectively. Changes in the array tilt only resulted in a modeled ±1°C average temperature, with azimuths around 240° generally producing the highest values. Thus, the change in azimuth was expected to increase the maximum temperature while not significantly affecting the average temperature.

The NC-EVA thin-film mock module exposed in Golden, Colorado, was mounted at a 180° azimuth (due south) and 40° latitude tilt [12] for aging in a moderately warm Steppe climate. For both the thin-film and silicon module types, this resulted in maximum measured temperatures between 102° and 104°C in Mesa, Arizona, and 93.5°C for the NC-EVA module in Golden, Colorado. The maximum temperatures measured in Arizona were very close to those predicted from the TMY3 data.

Mock module creep measurement

For the thin-film mock modules, the creep (displacement of the front glass relative to the back glass) was measured using a high-precision depth gauge, with 1-μm increments. The gauge was mounted to a flat plate to ensure that it was positioned perpendicular to the side of the module and in the plane of the glass. Creep measurement reproducibility was better than ±20 μm, Figure 4. For the Si modules, creep was monitored by comparison of optical and electroluminescence (EL) images before and after exposure.

Indoor thermal stress

An identical set of thin-film mock modules and Si modules were exposed to heat in environmental chambers indoors. The highest-performing Si modules of each pair made were chosen for outdoor deployment. Only in the case of the TPO-4 modules was the issue of specimen selection significant. One of the cells was broken in the indoor exposed module during its manufacturing. Indoor aging was performed in an SPX Corp. (Thermal Product Solutions Division Charlotte, North Carolina.) T64RC-7.5 oven with active control of temperature, with the humidity unregulated after the laboratory ambient air was heated to chamber temperature. Indoor tests were therefore performed with the humidity less than ~15% relative humidity. The Si modules were placed vertically in the chamber resting on

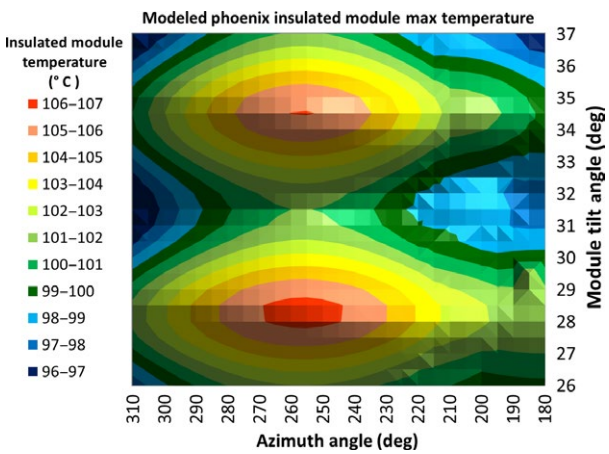

Figure 3. Maximum temperature predicted from TMY3 data and the King model [17] as a function of array tilt and azimuth angle (180° is due south).

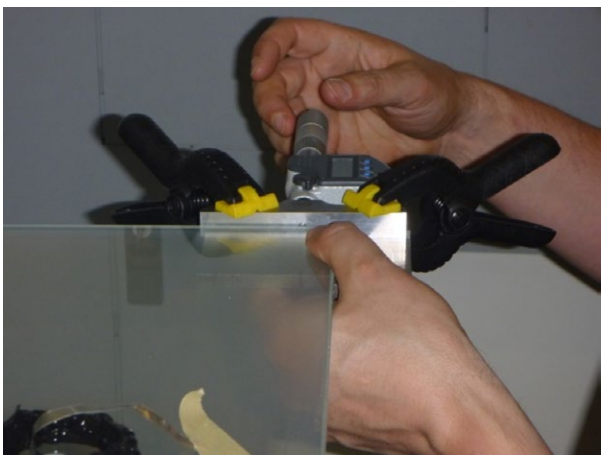

Figure 4. Photo of gauge used for measuring mock-module creep.

© 2015 The Authors. *Energy Science & Engineering* published by the Society of Chemical Industry and John Wiley & Sons Ltd.

their frames, with the junction box (J-box) toward the top (the same orientation as was used outdoors).

Knowing that NC-EVA and TPO-3 had significantly lower melting temperature and were therefore more likely to creep, we began testing these materials at 65°C for 200 h in a step-stress test. After each thermal exposure, current-voltage (IV) curves, photographs, and EL images were obtained for the Si modules; and creep measurements were made for the mock modules. All test specimens were then placed back in the chamber with the test temperature increased by 5°C, for another 200 h. When a temperature of 85°C was reached, all the remaining samples constructed with the other six encapsulants were placed in the chamber for the step-stress test.

The Si modules were tested up to a temperature of 110°C, at which point testing was stopped to preserve the modules in working condition for a subsequent experiment. In contrast, the mock modules continued to be heated in 10°C increments after the 110°C step, up to a final temperature of 140°C.

Results

Outdoor exposure temperatures

The temperature at the center of the Arizona modules, which were mounted to give the maximum temperatures possible, achieved values in the upper 90°C range, with small excursions up to between 102° to 104°C (Fig. 5). However, for the thermocouples mounted near the corners of the modules, the maximum temperatures were 15° to 20°C cooler. A similar histogram for the Colorado-deployed module produced temperatures with a maximum about 10°C cooler, but with a smaller, less pronounced peak at the highest temperatures. Both figures include the temperatures recorded during the night (typically the left of the figures) and day (right of the figures). The overall 10°C difference between the Arizona and Colorado data can be explained by the ~10°C higher ambient temperatures seen in Arizona. The peak in the high end of the Arizona module temperature data is attributed to the array orientation, where the highest irradiance from the sun occurs at the same time as the peak in ambient temperature. In Colorado, the module was oriented due south so that the peak solar irradiance occurred ~4 h before the greatest ambient temperature, flattening out the rightmost portion of module thermal profile.

Infrared (IR) images were taken to further qualitatively assess the temperature variation (Fig. 6A). For the crystalline-silicon module, a uniform temperature is observed within the module. The cooling around the perimeter is caused by better convective heat transfer and from efficient thermal conduction within the Al frame. Over the distance of 80 mm, that is, half a cell width, there is a 10°C change beyond which the temperature is uniform within ±2°C. For the thin-film mock module, there is less temperature variation between the sides of the module than between the top and bottom of the module (Fig. 6B). This is probably because of less insulation extending below and above the module than extends beyond the module at the sides (Fig. 2B). In all cases, the corner temperature was 15° to 20°C lower than the central temperature in both the IR images and the thermocouple histograms (Figs. 5 and 7); however, the majority

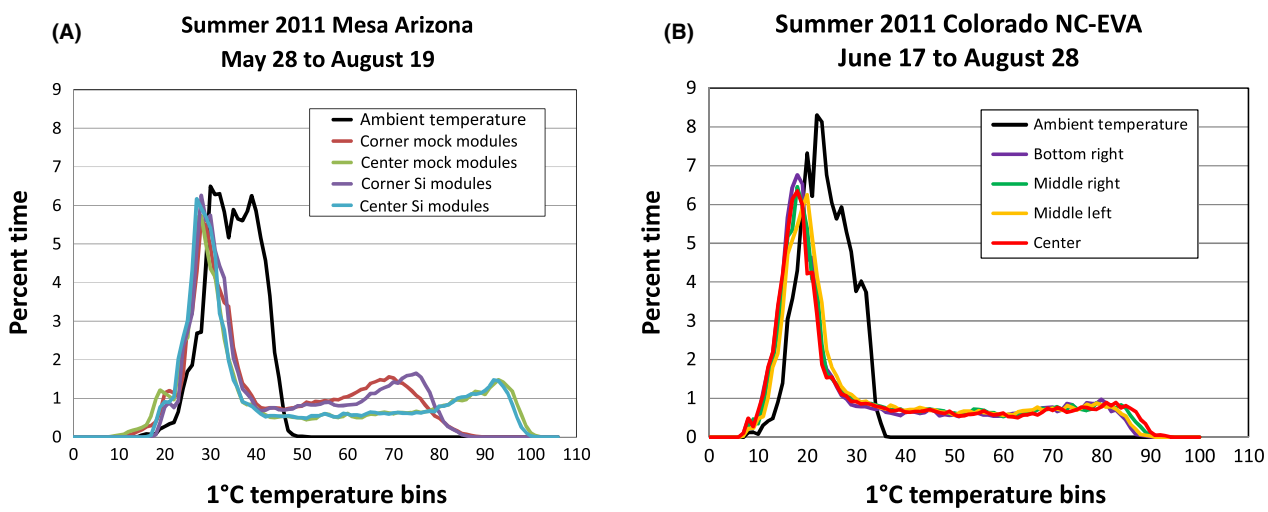

Figure 5. Summer temperature histograms for outdoor deployed modules. (A) Each profile represents the average of the eight modules for either the center or the corner thermocouple. Amongst each sample set, the individual histogram traces typically varied ±1°C or ±0.2%. (B) Histograms of four thermocouples placed on the Colorado-deployed NC-EVA mock module.

© 2015 The Authors. *Energy Science & Engineering* published by the Society of Chemical Industry and John Wiley & Sons Ltd.

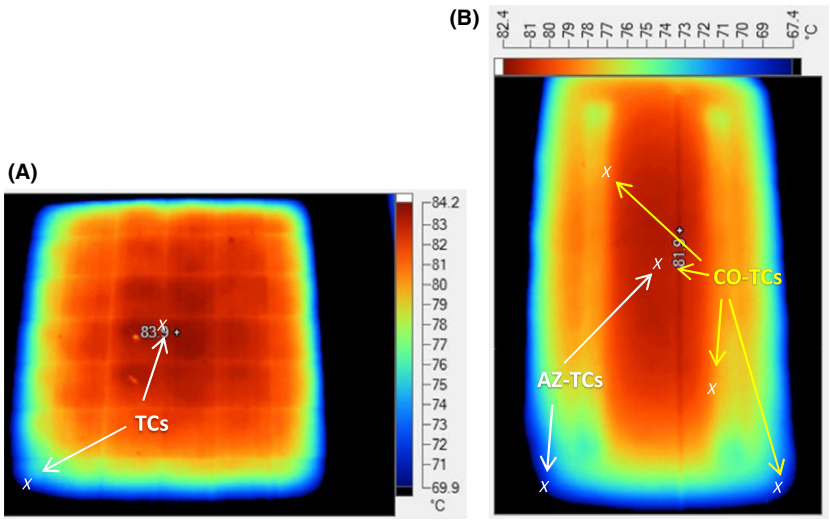

Figure 6. Infrared images of modules during deployment at the upper temperature ranges experienced. (A) Crystalline-silicon module temporarily set up in Colorado. (B) NC-EVA thin-film mock module deployed in Colorado. The locations of the thermocouples are indicated in the figure.

of the "active" region of modules is very close to the temperature indicated by the central thermocouple. Because the viscosity of a polymer can change rapidly near phase transitions and can have a strong variation in magnitude with temperature, the presence of a cooler perimeter could greatly affect the ability of the module to creep. A similar temperature differential appeared in both the thin-film mock and the crystalline-silicon modules, but the presence of an Al frame in the crystalline-silicon modules is expected to make it unlikely, but not impossible, to realize an installation configuration that would reduce this temperature heterogeneity significantly. It is this temperature differential that helps to significantly reduce the creep, despite most of the NC-EVA module being well above its melting point of around 65° to 69°C.

The modules were mounted individually, allowing air flow at the sides between modules, as opposed to a close-packed installation. Thus, it is possible to imagine an installation with modules mounted in a large array, on a flat rooftop, with higher temperatures or greater temperature uniformity than in Figures 5, 6, and 7. Furthermore, the record high temperature in Riyadh, Saudi Arabia, is 55°C—5°C hotter than the location of Phoenix—which would be expected to increase the module temperature by roughly 5°C in Riyadh.

However, the Si modules in Arizona were maintained open-circuited so that the 14.6% potential power output was converted to heat rather than electricity, as would be the case in an operating system drawing off power. To estimate the magnitude of this effect, we note that the maximum temperature of ~101°C for the NC-EVA module occurred when the ambient temperature was between 44.5° and 50°C. At elevated temperature, the

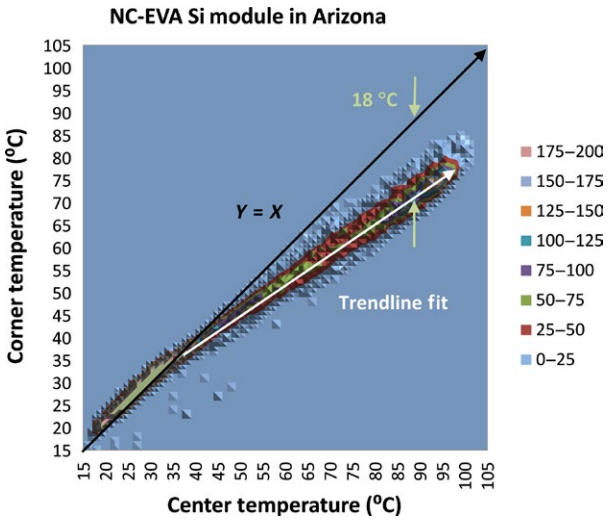

Figure 7. 2-D histogram of the center versus corner temperature of the NC-EVA Si module deployed in Arizona for the summer of 2011. The population of the data in 1 × 1°C bins is indicated in the figure legend.

14.6% module efficiency would be reduced by −0.5%/°C (relative), producing a module efficiency of ~9.4%. We estimate that this would reduce the ΔT of between ~56.5 and 51°C, to around 50°C above ambient for a maximum temperature of about 96°C if power was extracted from the module rather than converted to heat.

Modules are often mounted to encourage air flow. Even when building-integrated, a module is not likely to be mounted to a well-insulated roof surface (as chosen here to simulate a worst-case scenario) because such a configuration would run hot, compromising efficiency and PV durability [18–20]. We acknowledge that the high temperatures

© 2015 The Authors. *Energy Science & Engineering* published by the Society of Chemical Industry and John Wiley & Sons Ltd.

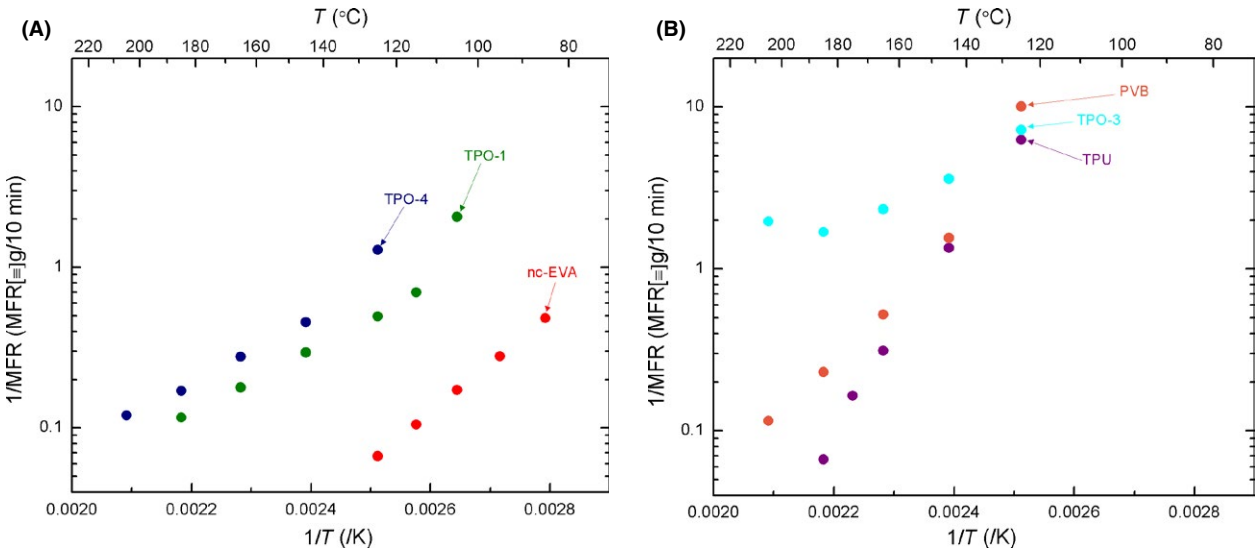

Figure 8. MFR results (with the linear Arrhenius fits shown) for (A) TPO-4, TPO-1, NC-EVA and (B) PVB, TPO-3, and TPU. Using the 4.23 kg test load.

in Figures 5 and 7, although rare, could exist for PV modules deployed at hot desert locations. Therefore, this experimental set-up is nearly the hottest possible configuration imaginable. Hotter installation would possibly run an additional 5° to 10°C hotter in a climate with a higher ambient temperature or for a significantly larger system where modules in the center of the arrays can get significantly hotter. However, to our knowledge, the hottest reported system temperatures do not exceed those of this study.

Inspection of the histograms (Figures 5 and 7) indicates that temperatures >100°C were experienced for a short amount of time (separately calculated at ~1 h), which over a 25 years lifetime of a module in Arizona would only sum to a total of around 25 h. The modules spent about 312 h at temperatures above 85°C over the course of the summer of 2011. The "damp-heat" qualification test runs at 85°C for 1000 h, that is, 3 years of exposure in Arizona. Similarly, in Colorado, the center of the module was above 85°C for only 57 h, that is, 1/18th of the duration of the damp-heat test. Thus, the current qualification test (1000 h at 85°C/85% RH) equates to a cumulative thermal exposure above 85°C that is less than observed in the most severe installations and potentially insufficient to evaluate the potential for creep.

Relative viscosity of materials by melt flow rate comparison

For the outdoor exposed modules, high-resolution optical photographs, EL, IV curves, and IR images were taken before and after exposure to look for creep and its effects. For all the modules, there were no overt signs of creep. However, it should be noted that the modules were mounted with cell strings running vertically, where the ribbon provides greatest mechanical support. If the Si modules had been mounted in the more mechanically compliant horizontal orientation, there may have been a greater likelihood for discernible creep to have occurred. Figure 8 shows the melt flow rate (MFR) measurements for the polymers used in this experiment. The relative values of the quantity 1/MFR should correspond to the relative values of the zero shear viscosity (the viscosity limit as the strain rate approaches zero) and to the relative expected amount of creep for the different materials. The NC-EVA crystalline-silicon module had the highest propensity to creep [12]. For the materials with melt transitions, the 1/MFR rose significantly beyond the range of measurement as the temperature is lowered near these transitions [12]. The viscous response of the NC-EVA near the upper limit of these experiments (~95°C) has a viscosity that would be expected to be several orders of magnitude lower than the other materials. Thus, if initial viscosity was the only consideration, one would expect the NC-EVA to creep orders of magnitude faster than the modules made using the other encapsulants [7].

Si module outdoor testing

As shown in Table 2, many of the modules, including TPO-1, TPO-3, TPO-4, and PDMS, experienced some performance losses after exposure in Arizona despite showing no visible signs of creep. Inspection of the EL images indicates this performance loss is coincident with the formation of cracks in the cells, Figure 9. The principal loss mode was through fill factor (*FF*), but because the modules have bypass diodes, the highest current-producing string

 © 2015 The Authors. *Energy Science & Engineering* published by the Society of Chemical Industry and John Wiley & Sons Ltd.

Table 2. Performance parameters for crystalline-silicon modules before and after aging. Uncertainty in these measurements is about 5% relative of the various reported values compared to actual, and ±0.5% for the values of the percent change. Yellow highlighted data are from modules where the EL images showed cracked cells. Module efficiency, open-circuit voltage, short-circuit current, fill factor, and maximum power are represented by the symbols η, V_{oc}, I_{sc}, *FF*, and P_{max}, respectively. Some numbers may be slightly inconsistent because of rounding.

Material and test location		Initial measurements					After Arizona exposure or 110°C environmental chamber exposure					%Change				
		η (%)	V_{oc} (V)	I_{sc} (A)	FF (%)	P_{max} (W)	η (%)	V_{oc} (V)	I_{sc} (A)	FF (%)	P_{max} (W)	η (%)	V_{oc} (V)	I_{sc} (A)	FF (%)	P_{max} (W)
EVA	Indoor	14.9	25.9	8.54	75.0	165	15.0	25.9	8.52	75.3	166	1.0	−0.1	−0.2	0.4	0.8
	ASU	15.1	26.2	8.54	75.0	168	15.1	26.2	8.41	76.1	168	−0.1	0.3	−1.5	1.4	0.1
NC-EVA	Indoor	14.9	26.0	8.54	75.0	166	15.0	25.9	8.51	75.7	167	0.5	−0.3	−0.4	0.9	0.8
	ASU	14.9	26.0	8.53	75.0	165	14.9	26.1	8.39	75.8	166	0.2	0.4	−1.7	1.1	0.3
TPU	Indoor	14.6	26.0	8.55	73.0	162	13.9	25.9	8.49	70.3	155	−4.8	−0.2	−0.7	−3.8	−4.6
	ASU	14.9	26.0	8.53	74.0	165	14.8	26.1	8.37	75.2	164	−0.4	0.3	−1.9	1.6	−0.5
PVB	Indoor	14.8	26.0	8.52	74.0	165	14.9	25.9	8.45	75.7	165	0.5	−0.4	−0.9	2.2	0.3
	ASU	14.9	26.0	8.53	75.0	166	14.8	26.2	8.39	75.1	165	−0.8	0.5	−1.7	0.1	−0.7
PDMS	Indoor	13.8	36.5	8.38	72.7	223	13.7	36.3	8.51	71.6	221	−0.7	−0.7	1.5	−1.5	−0.7
	ASU	13.9	36.7	8.43	72.9	225	13.6	36.6	8.39	71.4	220	−2.2	−0.1	−0.5	−2.1	−2.6
TPO-1	Indoor	14.8	26.0	8.45	75.0	164	14.9	26.0	8.47	75.5	166	0.7	−0.3	0.3	0.7	1.0
	ASU	14.2	25.9	8.51	72.0	158	13.8	26.0	8.46	69.7	153	−3.1	0.4	−0.6	−3.3	−3.1
TPO-3	Indoor	14.8	25.9	8.53	74.0	165	14.1	25.9	8.51	70.9	156	−5.0	0.0	−0.3	−4.4	−5.4
	ASU	14.9	26.0	8.50	75.0	165	12.3	26.2	7.97	65.5	137	−21	0.6	−6.7	−15	−21
TPO-4	Indoor	12.7	25.9	8.46	64.0	141	12.9	25.9	8.47	65.2	143	1.7	−0.2	0.1	1.8	1.4
	ASU	14.0	26.0	8.48	71.0	156	13.4	26.1	8.43	67.8	149	−4.5	0.5	−0.6	−4.7	−4.3

dominated the short-circuit current (I_{sc}) response, masking this degradation mechanism in most cases. Typically, *FF* loss was only a few percent stemming from only one or two cracked cells. Because cell cracking increases for high viscosity materials (compare Table 2 to Fig. 8), it is believed that the lamination of higher viscosity thermoplastic materials resulted in stressed cells that performed well initially but lost electrical connections later. This is evidenced by the much higher incidence of cell breakage during lamination of the TPO materials. However, it is also possible that higher modulus encapsulants could transfer more stress to cells, contributing to the increased breakage rate [2]. Although not statistically significant, it is noted that four of the six degraded modules were fielded in Arizona (the other two were stressed in the chamber), where they would have been exposed to prolonged thermal cycling and mechanical stresses, for example, wind load. Although encapsulant creep is not suspected to have significantly contributed to cell cracking, the results here indicate that, if lamination processes are not sufficiently optimized, higher viscosity encapsulant materials may mechanically stress cells during lamination (as was observed) or may facilitate crack formation during field deployment.

Mock module outdoor testing

Of the outdoor exposed modules, only the thin-film mock modules constructed using NC-EVA experienced significant creepage as measured when deployed, Fig. 10A. All the other encapsulants (Fig. 10B) showed no creep within the uncertainty of the outdoor measurements. When measured during field exposure, only two of the corners were readily accessible, and the presence of the insulation created additional difficulties, limiting the accuracy of measurements during exposure. Therefore, a more detailed and accurate laboratory measurement was made both before and after outdoor exposure, Figure 11. Here, the insulation was removed, allowing creep measurements to be performed at all four corners, improving the accuracy of the measurements. These indoor creep measurements indicated that the TPO-3 module crept 0.090 ± 0.036 mm and the TPO-1 module crept 0.032 ± 0.024 mm (Fig. 10). No creep was detected for the other encapsulants in the comprehensive final measurement. Even though most of the thermoplastic encapsulants reached either the melt or rubbery state within the module during exposure in Arizona (Table 1), no movement was observed. The melting and freezing transitions determined by DSC were only about 10°C higher or 4°C lower, respectively, for TPO-3 as compared to NC-EVA, Table 1. This demonstrates that the presence of a melt or glass transition is not sufficient to predict the potential for creep.

Noting the absence of creep beyond day 110 in AZ, where the maximum temperature did not exceed 90°C, and that the Colorado-deployed module barely crept while rarely reaching temperatures above 90°C indicates that creep

© 2015 The Authors. *Energy Science & Engineering* published by the Society of Chemical Industry and John Wiley & Sons Ltd.

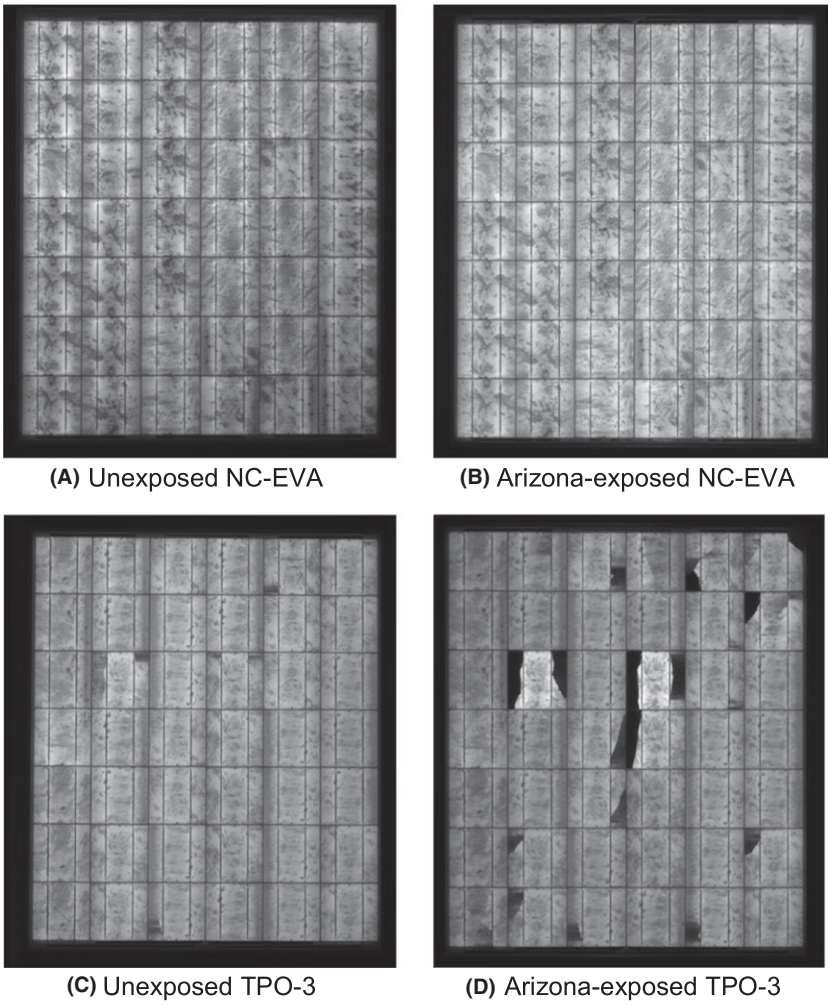

Figure 9. EL images of modules before and after exposure in Mesa, Arizona, at Arizona State University. (A) Unexposed module constructed with NC-EVA. (B) Arizona-exposed module constructed with NC-EVA. (C) Unexposed module constructed with TPO-3. (D) Arizona-exposed module constructed with TPO-3.

is possible for uncured EVA when the maximum module temperature approaches around 90°C, Figure 10. It is unlikely that one would expect to directly detect encapsulant creep in an outdoor-deployed module considering that: (1) module temperatures above 90°C will only occur in very hot environments when modules are mounted with very minimal air flow for heat transfer on the backside [21, 22], (2) significant temperature nonuniformities exist at the module periphery, restricting creep, (3) only the NC-EVA module, which has a very low viscosity, crept, and (4) the glass on these modules was unconstrained.

Over the first 30 days, creep was faster in the Arizona module (Fig. 10), but slowed down mid-summer despite the temperature being similar. Typical EVA formulations are known to crosslink as they age in the field [23]. This reduction in creep rate suggests that even without the peroxide additive, NC-EVA was crosslinking at these high temperatures in the field.

Mock module indoor testing

The MFR, Figure 8, which actually measures a rheological property, was not able to correctly rank order the materials in terms of creep. The value of 1/MFR is closely related to viscosity, but the presence of melt transitions produces large nonlinear changes in viscosity making extrapolation to operating conditions incorrect in these cases. Although TPO-1 and TPO-4 are much less viscous at temperatures above 120°C, TPO-3 is apparently much less viscous at module operating temperatures. Rheological properties used to assess the potential for creep must be measured at the module operating temperatures. The best rheological property to use for this purpose would be the zero shear viscosity.

Comparing Figures 11 and 12, more creep is seen in indoor experiments at lower temperatures relative to outdoor aging. Outdoors, the cool perimeter of the modules

 © 2015 The Authors. *Energy Science & Engineering* published by the Society of Chemical Industry and John Wiley & Sons Ltd.

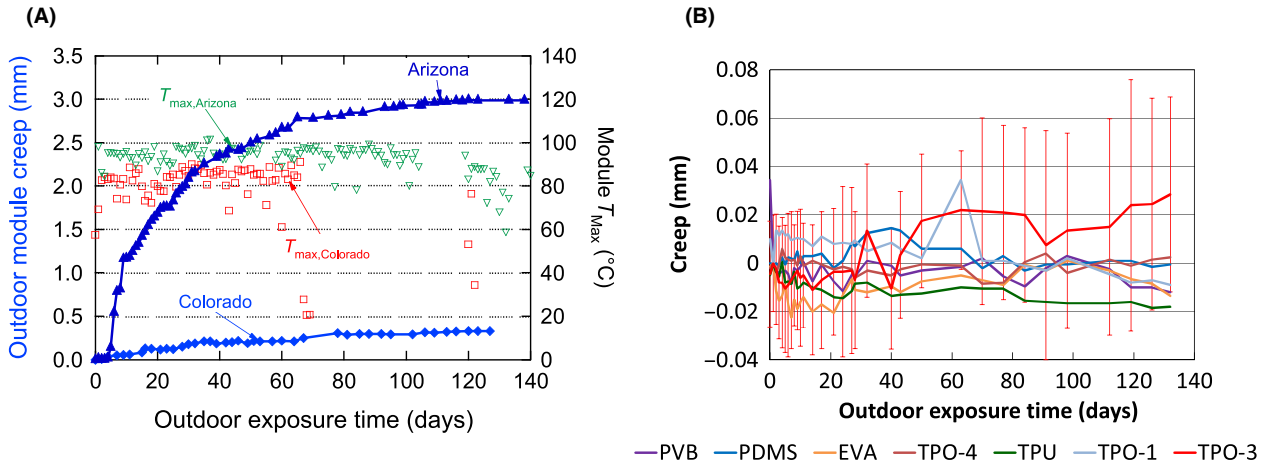

Figure 10. Measurement of thin-film mock module creep (relative displacement of top and bottom glass plates) during outdoor exposure. (A) Blue-creep distance, Green and Red-daily maximum module temperature in AZ and CO respectively. (B) Encapsulant types with relatively little to no creep. Error bars shown for TPO-3 only for clarity.

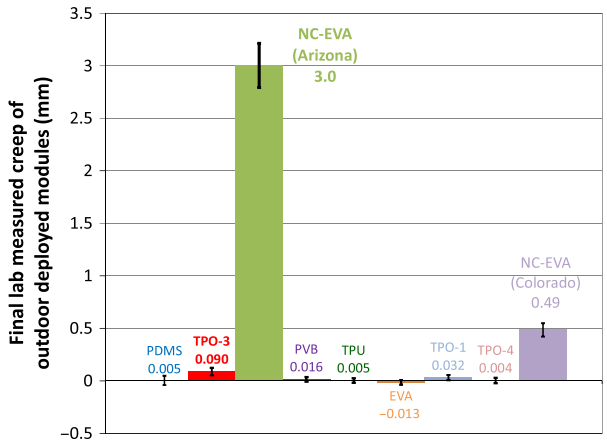

Figure 11. Measurement of thin-film mock module creep after field deployment in AZ or CO.

limits motion. In indoor testing, the NC-EVA began creeping detectably at 75°C in the thin-film mock module construction, and at 80°C in the crystalline-silicon construction. Similarly, the TPO-3 and TPO-1 thin-film mock modules began to creep detectably at 90° and 105°C, respectively. PVB goes through a glass transition at around 16°C with no melt transition, but did not begin to creep until it was well above 100°C. Creep in PVB was mitigated because of its greater viscosity [12]. DMA measurements indicate that the phase angle of PVB reaches 45°, the crossover point, at 121°C, which corresponds with its onset of creep in indoor aging. However, the TPU had a crossover at a much lower temperature than the onset of creep. These temperatures for the onset of creep correspond better to the temperatures determined by DMA than those determined by DSC, Table 1. This is because DSC is measuring the thermal effects of increased polymer mobility, but DMA is directly assessing the effect of phase transition on the bulk rheological properties.

The slope of the creep versus temperature curve for TPO-3 does not continue to increase rapidly beyond 95°C, suggesting that TPO-3 is chemically crosslinking at temperatures above 90°C. At temperatures above 110°C, the amount of creep in each cycle begins to decrease for TPO-3. Similar behavior is also seen for TPO-1, TPO-4, and PVB. The crosslinking and/or chain scission of these materials was characterized using gel-content measurements and multiangle laser light-scattering. This will be the topic of a subsequent paper.

In indoor testing, the TPU and the NC-EVA showed a continually increasing creep rate with increasing temperature. For NC-EVA, testing had to be stopped at 75°C because of excess creep, and we were not able to test at sufficiently high temperatures where the crosslinking chemistry was fast enough. The TPU similarly crept more than 1 cm at 125°C, contacting the chamber floor, preventing higher temperature exposure (see the dashed arrow in Fig. 12 for TPU). Bubbles began to form within the TPU module at 105°C and became located throughout the module after exposure at 110°C. The TPU is suspected to be unique in rapidly chemically decomposing at elevated temperatures. This decomposition may also explain the onset of creep is not coincident with the crossover temperature of 85°C.

Measuring the change in creep during a given testing step (Fig. 12B) is similar to measuring the reciprocal of the zero shear viscosity at the test temperature. Initially, as the temperature is increased, the creep rate increases; but at higher temperatures, the creep rate decreases, suggesting crosslinking of the materials, similar to the outdoor

© 2015 The Authors. *Energy Science & Engineering* published by the Society of Chemical Industry and John Wiley & Sons Ltd.

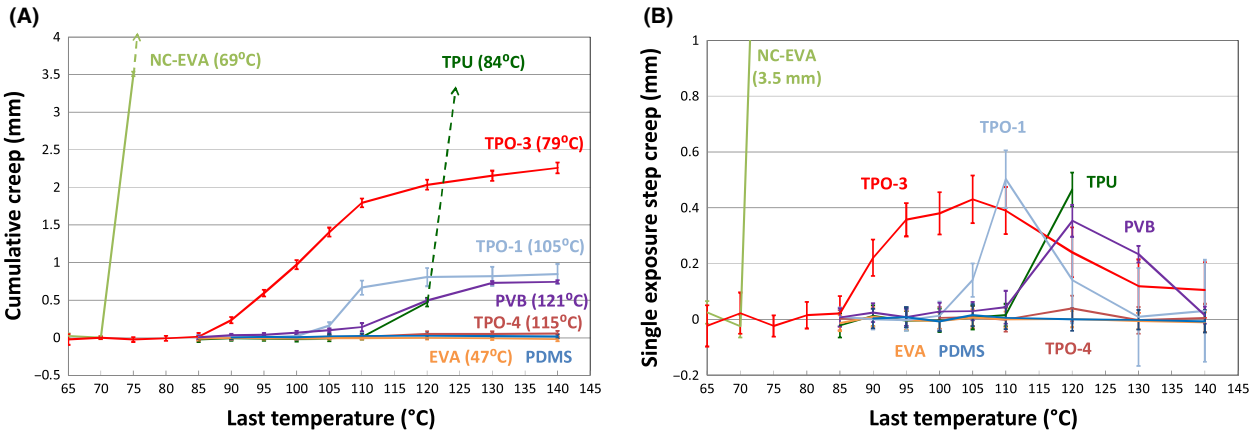

Figure 12. (A) Relative displacement of glass sheets in the thin-film mock modules after step-stress aging, of a duration of 200 h each. The indicated temperatures are the DMA-determined T_m or T_c from Table 1. (B) Creep experienced during a 200-h step stress cycle at the given temperature.

fielded mock modules. Noting that in the fielded modules, NC-EVA crept several mm, TPO-3 crept 0.9 mm, and TPO-1 only crept a barely detectable amount, the evaluation of zero shear viscosity at temperatures between 90° and 105°C would provide a prediction of initial creep during outdoor use. If such a test were extended for a long period of time, it could also highlight the tendency of a material to crosslink in response to heat, limiting the amount of creep.

Crystalline-silicon module indoor testing

In indoor studies, the onset of creep for the NC-EVA silicon module occurred at 75°C (Fig. 12A). Here, despite the fact that the sides of adjacent rows of cells appeared to touch, there was no discernible performance loss with step stress tests up to 100°C, (Fig. 13A and B, Table 3). Even though this significant cell movement did not directly create a performance issue, it could cause a ground-fault safety issue, and it is likely that subsequent exposure to thermal cycling would increase the mechanical stress on the tabbing and solder bonds, increasing the long-term failure rates.

Wet insulation resistance

Despite creeping 3 mm, the outdoor-exposed NC-EVA mock module still passed the wet high-pot test. For all outdoor-exposed modules, the wet high-pot resistance was constant (within uncertainty) or increased upon exposure. However, some of the samples showed resistances >10,000 MΩ, the measurement limit for the instrument.

Table 3. Results of wet high-pot testing according to IEC 61730. Pass criterion is 40 MΩ/m^2.

	Arizona or Colorado outdoor deployment				Environmental chamber stress testing			
	Mock module		Crystalline Si module		Mock module		Crystalline Si module	
	Before exposure	After exposure	Before exposure	After exposure	Before exposure	After exposure	Before exposure	After exposure
Encapsulant type	(MΩ)	(MΩ)	(MΩ)	(MΩ)	(MΩ)	(MΩ)	(MΩ)	(MΩ)
Allowable Limit	57 (MΩ)		36.4 or 24.7 (MΩ)		57 (MΩ)		36.4 or 24.7 (MΩ)	
EVA	>10,000	>10,000	110	170	160	>10,000	100	190
NC-EVA	160	250	110	100	210	**<1**	100	140
PDMS	350	>10,000	1500	2500	290	350	1300	740
TPO-1	290	340	>10,000	>10,000	9100	390	>10,000	>10,000
TPO-3	250	360	1400	2800	300	380	1400	4100
TPO-4	360	>10,000	>10,000	>10,000	300	**Cracked**	>10,000	>10,000
PVB	160	690	65	61	110	**Cracked**	70	66
TPU	190	>10,000	150	130	270	**<1**	170	160
EVA (Colorado)	100	270						

Values in bold print are for modules that failed the wet high-pot test.

© 2015 The Authors. *Energy Science & Engineering* published by the Society of Chemical Industry and John Wiley & Sons Ltd.

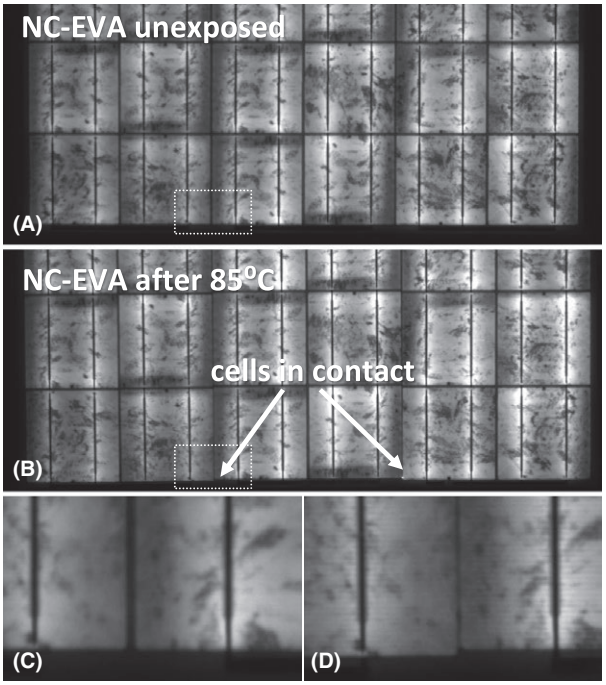

Figure 13. Electroluminescent images of the NC-EVA crystalline Si (A) before thermal exposure and (B) after the 85°C exposure step of the indoor step-stress test. (C, D) Detail from the bottom row of the module, insets as indicated by the boxes in A and B, respectively.

The wires for connecting to the TCO were not soldered, but were adhered to the TCO using a pressure-sensitive adhesive. The bond area is 0.635 cm × 107 cm (68 cm^2), but poor electrical contact was possible. The TPO-1 and TPO-4 crystalline Si modules also occasionally demonstrated high, >10,000 MΩ, resistances, where the presence of a measurable IV curve indicates that electronic contact was obtained.

For the case of a mock module with a high-resistance polymer and a sufficient edge delete, the resistance through the glass was ~360 MΩ. For a 3.18-mm-thick glass, with a TCO area defined by the module size minus the edge-delete region, corresponding to a volume resistivity of glass of 7.9×10^{12} Ω·cm. The estimated volume resistivity is higher than typical literature values (~10^{11} Ω·cm) [24], probably due to the use of SiO_2 layers next to the TCO. Therefore, any values significantly higher than 360 MΩ indicate some loss of electrical contact. Values lower than 360 MΩ indicate significant current through the encapsulant, poor edge delete, or loss of adhesion somewhere within the package. Considering that the NC-EVA modules crept the most and were the only ones to show visible signs of flow, a large amount of creep (a few mm) can be tolerated before an immediate safety concern would appear in either module construction type. We only detected failure of the wet high-pot test for samples with cracked glass or which experienced creep >1 cm.

Discussion: Creep and its Consequences

In addition to encapsulant properties, the module construction is an important factor to consider for creep. None of the crystalline Si modules demonstrated measureable creep when deployed outdoors. Despite approaching the maximum temperatures possible for a fielded module, none of the crystalline Si modules experienced a detectable safety or performance failure due to the use of a thermoplastic encapsulant. However, the modules were mounted with the cell strings arranged vertically, which may have reduced the propensity for the cells to be displaced.

Even though no movement was seen in the NC-EVA crystalline Si module, it is possible that movement on the order of 100 μm may have occurred. Such movement could put some additional mechanical stress on the interconnects (solder joints and ribbons) that might take years of aging (thermal and/or mechanical cycling) to yield an overt effect. If problems with undercured EVA exist, they are not likely to be a common occurrence, noting that (1) NC-EVA represents an extreme level of undercure, (2) the EVA will cure in time [23], (3) modules may have some level of tensile stress in them from the lamination process anyway, and (4) these modules were exposed to extreme conditions of heat. The study here predominantly applies to infant mortality—within the first few years of field exposure—and does not attempt to examine more prolonged aging.

The lesser creep in the Si modules relative to the mock modules can foremost be attributed to the fact that the polymeric backsheet is held in place by the frame, restricting component movement. Similarly, a typical thin-film module might be constructed using either a frame, or clips on the edges for mounting. Either of these package configurations would mitigate creep. If the glass in a thin-film module is fixed, only a few busbars within the encapsulant would be able to move, which would only happen in a very low-viscosity encapsulant. In this case, the more likely scenario is that flow would probably not directly affect the performance; but with sufficient time, polymer may flow out of the bottom of the module, creating a safety concern. Thus, an encapsulant would typically need to have a viscosity much lower than NC-EVA in Table 1 to pose an immediate safety or performance issue.

Within the PV industry, there is much attention to control of the degree of cure of the encapsulant during module processing. Some of this concern is because of

© 2015 The Authors. *Energy Science & Engineering* published by the Society of Chemical Industry and John Wiley & Sons Ltd.

potential problems due to module creep [1] and with poor adhesion during the qualification tests. This study has shown that even a nonperoxide-containing EVA would not be expected to pose a significant risk for prolonged creep. If fielded, an incompletely cured EVA module would be likely to cure in time with exposure to UV light and humidity. Fielded EVA modules typically have gel contents greater than 90%, despite not being initially cured to that level [1, 9, 23, 25]. However, for a module to pass the qualification tests, the amount of crosslinking is important. For example, in Figure 13, the cells were displaced enough that it is possible for a module to fail the visual inspection if this reduced a critical clearance distance or caused some components to contact each other even though the performance of the crystalline Si module was not decreased.

Many in the PV field have identified that an incompletely cured or improperly cured module might not have good adhesion retention [26]. This may occur, for example, if the peroxide crosslinking agent also functions to activate an adhesion-promoting compound. The current study indicates that concerns with adequate processing, as measured by gel content, are more likely to apply to adhesion retention than to component displacement.

The tests here were conducted to examine modules fielded at the highest temperatures expected for PV systems integrated into a well-insulated roof. Rack-mounted modules would clearly be expected to have a temperature ~15°C lower [17] than building-integrated or building-applied PV systems [21, 22]. The only ways to achieve higher temperatures would be if: modules were mounted in an even hotter environment than Phoenix, AZ, were mirror-augmented, mounted near a heat source such as a vent, or part of a much larger building-integrated array and mounted with no convective cooling on the backside on a well-insulated roof.

This study examined a few emerging candidate encapsulant materials, but the possibility still exists that a newer material may experience thermally induced failure modes (including creep) that might not be screened in the current qualification test methods. Consider that the maximum module temperature of 105°C is not examined within the present module qualification tests. Because the amount of time at temperatures above 85°C is very limited, a relatively short test at high temperature should be able to screen the majority of these failure modes. Therefore, it has been proposed to IEC to subject modules to a temperature of 105°C for 200 h as part of IEC 61215. Because it is likely that when deployed there may be cool spots restricting flow, this test represents a test with a significant safety factor. This proposal, in addition to hot-spot testing, would screen for components and adhesives that might creep at temperatures above 85°C.

Conclusions

The use of 85°C and humidity freeze cycles (amongst other tests) in IEC standards necessitates crosslinking of typical EVA formulations to achieve gel contents in excess of around 65% to provide adequate adhesion properties and resistance to creep. However, this work indicates that even if an EVA encapsulant was formulated without peroxides to form chemical crosslinks, virtually no creep would be expected to be seen outdoors with typical module constructions and mounting. Only modules with an unrestrained front-glass were shown to have any propensity to creep outdoors. This absence of creep observations in fielded modules is due, in part, to the nonuniformity of temperature resulting in small lower-temperature areas that significantly resist creep, and to the restricted motion of front and backsheets by frames and mounting clips.

The materials tested produced creep profiles that indicate formation of crosslinks in response to heat and UV light or to heat only despite the presence of a polymer stabilizing formulation and in the absence of peroxides or other curing agents. Evidence was also presented that NC-EVA, TPO-1, and TPO-3 thermally crosslink despite the absence of peroxide above temperatures above ~100°C. This unintended crosslinking actually serves to further mitigate the potential for creep in some materials.

Often, researchers will consider the temperature of melting or glass transitions when estimating the likelihood of material creep. However, this work indicates that the onset of creep coincides reasonably well to the melting (or crossover) points determined by DMA using the phase angle of 45°, but not so well to the phase transitions indicated by DSC (compare Table 1 to Fig. 12). So when evaluating materials for the likelihood of creep, one must assess relevant rheological properties at the temperatures of interest. The zero shear viscosity would be the best predictor, but DMA-determined melting or crossover points are good indicators of potential problems.

Once the encapsulant has been chosen, quick screening tests could be performed to evaluate creep as a module test. To ensure adequate performance, it has been proposed to expose modules to 200 h at 105°C as part of IEC 61215. In general, the probability of module creep being significant is very low compared to other risks.

Acknowledgments

This work was part of a collaborative effort of a number of people contributing to test standard development at many institutions. The authors gratefully acknowledge the support of the following individuals: Adam Stokes, Alain Blosse, Ann Norris, Bernd Koll, Bret Adams, Casimir Kotarba (Chad), David Trudell, Dylan Nobles, Ed Gelak,

 © 2015 The Authors. *Energy Science & Engineering* published by the Society of Chemical Industry and John Wiley & Sons Ltd.

Greg Perrin, Hirofumi Zenkoh, James Galica, Jayesh Bokria, John Pern, Jose Cano, Kartheek Koka, Kate Stika, Keith Emery, Kent Terwilliger, Kolapo Olakonu, Masaaki Yamamichi, Mowafak Al-Jassim, Nick Powell, Niki Nickel, Pedro Gonzales, Peter Hacke, Ryan Smith, Ryan Tucker, Steve Glick, Steve Rummel, Tsuyoshi Shioda, and Yefim Brun. This work was supported by the U.S. Department of Energy under Contract No. DE-AC36-08-GO28308 with the National Renewable Energy Laboratory.

Conflict of Interest

None declared.

References

1. Cuddihy, E. F., A. Gupta, C. D. Coulbert, R. H. Liang, A. Gupta, P. Willis, et al. 1983. Applications of ethylene vinyl acetate as an encapsulation material for terrestrial photovoltaic modules. DOE/JPL/1012-87 (DE83013509). Pasadena, California.
2. Dietrich, S., M. Pander, M. Ebert, and J. Bagdahn. 2008. Mechanical assessment of large photovoltaic modules by test and finite element analysis. 23rd European Photovoltaic Solar Energy Conference. Valencia, Spain.
3. Wohlgemuth, J., M. Kempe, D. Miller, and S. Kurtz. 2011. Developing standards for PV packaging materials. SPIE, San Diego, California.
4. Wohlgemuth, J., and W. Herrmann. 2005. Hot spot tests for crystalline silicon modules. 31st IEEE Photovoltaic Specialists Conference. pp. 1062-1063, 3–7 January 2005. ISSN 0160-8371, Lake Buena Vista, Florida.
5. Wohlgemuth, J. 2013. Hot spot testing of PV modules. SPIE, San Diego, California.
6. Kurtz, S., K. Whitfield, D. Miller, J. Joyce, J. H. Wohlgemuth, M. D. Kempe, et al. 2009. Evaluation of high-temperature exposure of rack-mounted pohotovoltaic modules. 34th IEEE PVSC. Philadelphia, Pennsylvania.
7. Miller, D. C., M. D. Kempe, S. H. Glick, and S. R. Kurtz. 2010. Creep in photovoltaic modules: Examining the stability of polymeric materials and components. 35th IEEE Photovoltaic Specialists Conference (PVSC), 20–25 June 2010. Honolulu, HI.
8. Cuddihy, E. F., and P. B. Willis. 1984. Antisoiling technology: theories of surface soiling and performance of antisoiling surface coatings. DOE/JPL/1012-102 (DE85006658), Pasadena, California.
9. Holley, W. W., and S. C. Agro. 1998. Advanced EVA-based encapsulants, Final Report January 1993-June 1997. NREL/SR-520-25296, Golden, Colorado.
10. Ehrich, C., S.-H. Schulze, I. Hinz, M. Pander, and M. Ebert. 2011. Development of a novel technique for mechanical characterization of polymer encapsulantes in laminated glass beams. 26th European Photovoltaic Solar Energy Conference and Exhibition. Pp. 3560–3565, Hamburg, Germany.
11. Kempe, M. D., D. C. Miller, J. H. Wohlgemuth, S. R. Kurtz, J. M. Moseley, Q.-U.-A. S. J. Shah, et al. 2012. A field evaluation of the potential for creep in thermoplastic encapsulant materials. Proceedings of the 38th IEEE Photovoltaic Specialists Conference. Austin, Texas.
12. Moseley, J. M., D. C. Miller, Q.-U.-A. S. J. Shah, K. Sakurai, M. D. Kempe, G. TamizhMani, et al. 2011. The melt flow rate test in a reliability study of thermoplastic encapsulation materials in photovoltaic modules. NREL/TP-5200-52586. Pp. 1–20, Golden, Colorado.
13. IEC, 61215, Crystalline silicon terrestrial photovoltaic (PV) modules - Design qualification and type approval. ed: Ed. 2. 2005.
14. UL 1703, Standard for Safety for Flat-Plate Photovoltaic Modules and Panels. 2002.
15. IEC, 61730,Photovoltaic (PV) module safety qualification - Part 1: Requirements for construction. ed: Ed. 1.0. 2004.
16. ASTM G173-03, Standard tables for reference solar spectral irradiances: direct normal and hemispherical on 37 tilted surface. 2012.
17. King, D. L., W. E. Boyson, and J. A. Kratochvil. 2004. Photovoltaic Array Performance Model. SAND2004-3535. Sandia National Laboratories, Albuquerque, NM.
18. Shrestha, B. L., E. G. Palomino, and G. TamizhMani. 2009. Temperature of rooftop photovoltaic modules: air gap effects. Proceedings of the SPIE - The International Society for Optical Engineering. San Diego, California.
19. Jaewon, O., and G. TamizhMani. 2011. BAPV modules: Installed-NOCT and temperature coefficients after 1-year exposure. 37th IEEE Photovoltaic Specialists Conference (PVSC), 000838-000841, 19–24 June 2011. Seattle, Washington.
20. Hrica, J., S. Chatterjee, and G. TamizhMani. 2011. BAPV array: thermal modeling and cooling effect of exhaust fan. Pp. 003144–003149 Photovoltaic Specialists Conference (PVSC). 37th IEEE. Seattle, Washington.
21. Chatterjee, S., and G. TamizhMani. 2012. BAPV arrays: Side-by-side comparison with and without fan cooling. 38th IEEE Photovoltaic Specialists Conference (PVSC), 537-542, 3–8 June 2012, Austin, Texas.
22. Hrica, J., S. Chatterjee, and G. TamizhMani. 2011. BAPV array: Thermal modeling and cooling effect of exhaust fan. 37th IEEE Photovoltaic Specialists Conference (PVSC), 3144-3149, 19–24 June 2011. Seattle, Washington.
23. Pern, F. J., and A. W. Czanderna. 1992. Characterization of ethylene vinyl acetate (EVA) encapsulant: effects of thermal processing and

© 2015 The Authors. *Energy Science & Engineering* published by the Society of Chemical Industry and John Wiley & Sons Ltd.

weathering degradation on its discoloration. Sol. Energy Mater. Sol. Cells 25:3–23.

24. Seddon, E., E. J. Tippett, and W. E. S. Turner. 1932. The Electrical Conductivity of Sodium Metasilicate-Silica Glasses. J. Soc. Glass Technol. 16:450–477.
25. Klemchuk, P., M. Ezrin, G. Lavigne, W. Holley, J. Galica, and S. Agro. 1997. Investigation of the degradation and stabilization of EVA-based encapsulant in field-aged solar energy modules. Polym. Degrad. Stab. 55:347–365.
26. Chapuis, V., S. Pélisset, M. Raeis-Barnéoud, H.-Y. Li, C. Ballif, and L.-E. Perret-Aebi. 2014. Compressive-shear adhesion characterization of polyvinyl-butyral and ethylene-vinyl acetate at different curing times before and after exposure to damp-heat conditions. Prog. Photovoltaics Res. Appl. 22:405–414.

 © 2015 The Authors. *Energy Science & Engineering* published by the Society of Chemical Industry and John Wiley & Sons Ltd.